Hindawi
Wireless Communications and Mobile Computing
Volume 2022, Article ID 8553845, 7 pages
https://doi.org/10.1155/2022/8553845

Research Article

A Novel Modulation Technique with Low PAPR for 5G-IoT Systems

Junchao Sun, Buyu Chen, Ding Huang, Baobing Wang, Tian Xiang, and Dejin Kong

State Key Laboratory of New Textile Materials and Advanced Processing Technologies, The School of Electronic and Electrical Engineering, Wuhan Textile University, Wuhan 430200, China

Correspondence should be addressed to Dejin Kong; djkou@wtu.edu.cn

Received 13 May 2022; Accepted 10 July 2022; Published 25 July 2022

Academic Editor: Han Wang

For existing orthogonal frequency division multiplexing (OFDM) in 5G internet of things (5G-IoT) systems, one of the critical problems is the high peak to average power ratio (PAPR), which seriously degrades the energy efficiency. To this end, we propose a novel modulation technique with low PAPR for IoT systems, which preserves the advantage of low implementation complexity and ability to fight against multipath channels. The key methodology is the employment of symbol repetition in the frequency domain. Hence, by designing the appropriate phase factors on the repeated symbols, the PAPR of transmitted signals is equivalent to that of an OFDM signal with a reduced size of discrete Fourier transform (DFT). It is demonstrated that, even if there exists repetitive symbols, the proposed method can still maintain an unreduced spectral efficiency performance. Moreover, to evaluate the proposed method, the Monte-Carlo simulations are conducted for the complementary cumulative distribution function (CCDF) and the bit error rate under multipath fading channels. The simulations show that, as CCDF = 10^{-3}, the proposed method can achieve 2.5 dB gains about the PAPR compared with the original OFDM signal.

1. Introduction

In recent years, 5G-enabled internet of things (5G-IoT) have attracted much attention due to the features of low cost, low power consumption, and wide coverage, which put forward a challenge on the modulation technique. As it is well known, orthogonal frequency division multiplexing (OFDM) is one classical modulation technique and has been widely applied in many communication standards due to the low implementation complexity and ability to fight against multipath channels [1–3]. However, as one of multicarrier modulations, OFDM suffers from the problem of high peak to average power ratio (PAPR), which severely impairs the efficiency of power amplifiers and is unfavourable for the features of low power consumption and wide coverage. Consequently, OFDM may be not an optimal candidate for 5G-IoT systems.

Up to now, various approaches have been proposed to address the PAPR reduction in OFDM systems. These methods are divided into two main categories. One category requires the advance transmission of side information (SI), which costs precious time-frequency resources in control channels generally. For example, the selective mapping (SLM) method was considered in [4], and the partial transmit sequence (PTS) was proposed in [5]. In addition, high complexity is another main drawback for the selected SLM and PTS methods due to the optimal selection from multiple phase sequences. Another category of PAPR reduction methods [6–10] is SI-free approaches. In [6], the PAPR was reduced by directly clipping the transmitted signal, at the cost of degrading the performances of bit error rate (BER) and out-of-band radiation. In [7], the tone reservation method was presented to reduce the PAPR using a peak-canceling signal that generated a set of reserved tones, in which the reservation of tones reduced the spectral efficiency. In [8], an extended SLM was proposed for the PAPR reduction without SI by constructing extension matrices comprising amplitude extensions and phase rotations. In [9], a polar coding-based SI-free SLM scheme was presented by constructing coset codes of a linear polar code, and meanwhile, an adaptive trial-based blind receiver was presented for detection of the selected signal. In [10], the authors proposed a blind interleaving technique with signal space diversity, which reduces the PAPR in OFDM significantly without the need of SI.

In this paper, a novel modulation technique with low PAPR is proposed for 5G-IoT systems, in which the key methodology is the employment of symbol repetition. By designing the appropriate phase factors on the repeated symbols, the PAPR of transmitted signals is equivalent to that of an OFDM signal with a reduced size of discrete Fourier transform (DFT). With the proposed method, the peak power of the transmitted signal is low, without the signal distortion and the need of SI. Furthermore, although the proposed scheme employs the design of symbol repetition, the spectral efficiency can be maintained since the same amount of symbols is transmitted. To evaluate the proposed scheme, simulations are conducted to obtain the curves of the complementary cumulative distribution function (CCDF) and BER under multipath fading channels.

Through this paper, the remainder is organized as follows. In Section 2, the system model of OFDM is introduced. Then, the novel modulation technique is presented for 5G-IoT in Section 3, and the PAPR performance is analyzed in Section 4. Subsequently, simulation results are given in Section 5. Finally, Section 6 gives the conclusion.

2. System Model

In this section, an OFDM system is introduced briefly, in which x_m stands for the transmitted symbol of m-th subcarrier. By considering the signal superposition of M subcarriers, the transmitted signal is obtained and the transmitted signal of the OFDM system is expressed as [11, 12]

$$s(k) = \frac{1}{\sqrt{M}} \sum_{m=0}^{M-1} x_m e^{j2\pi mk/M}, \quad k = 0, 1, \cdots, M-1. \tag{1}$$

Subsequently, to overcome multipath channels, cyclic prefix (CP) is inserted in front of each symbol, which converts the multipath channels into a coefficient for each subcarrier. At the receiver side, after removing CP and carrying out M-point discrete Fourier transform (DFT), symbol demodulation is given as

$$y_m = H_m x_m + \eta_m, \quad m = 0, 1, \cdots, M-1, \tag{2}$$

where H_m is the channel coefficient for the m-th subcarrier and η_m is the Gaussian noise with zero mean and variance σ^2 [13].

Finally, symbol recovery is easily conducted by the single-tap equalization when it is available for the receiver, i.e.,

$$\widehat{x}_m = \frac{y_m}{H_m}. \tag{3}$$

Then, we focus on the problem of high PAPR in OFDM, which has a critical influence on the power amplifier efficiency in wireless communications. The definition of PAPR in OFDM is given as

$$\text{PAPR} = \frac{\max_{0 \le k < M} |s(k)|^2}{\mathbb{E}\left[|s(k)|^2\right]}, \tag{4}$$

where $\mathbb{E}[\cdot]$ is the expectation operator. Note that the averaging transmitting power $\mathbb{E}[|s(k)|^2]$ is equivalent to the averaging power of x_m due to the reason that $s(k)$ is the inverse DFT (IDFT) of x_m. When the averaging power of x_m is equal to 1, the value of $\mathbb{E}[|s(k)|^2]$ will be 1. Therefore, the value of PAPR is determined by the fluctuation of the transmitted signal. As is well known, the fluctuation of the signal in OFDM becomes stronger as the subcarrier number grows, especially when the total subcarrier number is limited. As a result, OFDM systems with a larger subcarrier number usually exhibit a larger PAPR.

3. Proposed Modulation Technique with Low PAPR

In this section, a novel modulation technique with low PAPR is proposed for 5G-IoT systems. The key idea is the employment of symbol repetition in the frequency domain. SI is not required, and the low complexity is observed in the proposed method, which makes it preferred in practice. As a remark, the concept of symbol repetition has been also applied in filter-bank multicarrier for the interference cancellation [14, 15].

In the proposed scheme, the whole M subcarriers in OFDM are divided into P groups and each group consists of $R = M/P$ subcarriers. The transmitted symbols in each group are the same; i.e., symbols are repeated in each group. To maintain the same data rate, more branches can be designed to transmit symbols, and the number of branches is the same as the number of the groups.

Let $d_{m,p}$ denote the transmitted symbol, where $m \in [0, M-1]$ is the subcarrier index and $p \in [0, P-1]$ is the branch index. Different p stands for different branch. Figure 1 depicts the transmitter of different branch by changing the value of p.

The transmitted symbols in each group are the same, i.e.,

$$d_{r,p} = d_{nR+r,p}, \tag{5}$$

where $r = 0, 1, \cdots, R-1$ and $p, n \in [0, P-1]$. In other words, the symbols $d_{r,p}$ are transmitted repeatedly in the frequency domain. Note that the original data symbols x_m are divided into P groups, and the p-th group is transmitted via the p-th branch in the proposed scheme; i.e., x_{pR+r} corresponds to $d_{m,p}$. It is worthwhile to point out that p in $d_{m,p}$ is the branch index, not the time index. The symbols $d_{m,p}$ for different p can be simultaneously transmitted. During one symbol duration, total RP, i.e., M, symbols can be transmitted in the proposed scheme, exactly as the classical OFDM systems.

As one multicarrier modulation, the OFDM's orthogonality is very important, and on this basis, no interference among symbols is caused. To avoid interference among symbols, it is still important to maintain orthogonality in the proposed scheme. To maintain the orthogonality between $d_{m,p}$ for different p, transmitted symbols, $d_{m,p}$, are multiplied by the orthogonal phase sequences. For the k-th group, after

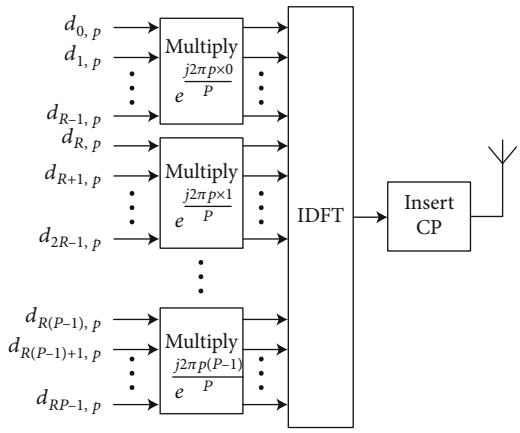

Figure 1: The transmitter of the proposed scheme.

multiplying the phase sequences, we get

$$\bar{d}_{nR+r,p} = d_{nR+r,p} e^{j2\pi np/P}, \tag{6}$$

where $p \in [0, P-1]$. Note that $nR + r$ is the subcarrier index and $nR + r \in [0, M-1]$.

Next, M-point IDFT is performed on $\bar{d}_{kR+r,p}$, which gives

$$s_p(k) = \frac{1}{\sqrt{M}} \sum_{m=0}^{M-1} \bar{d}_{m,p} e^{j2\pi mk/M}, \quad k = 0, 1, \cdots, M-1. \tag{7}$$

Since symbols $d_{m,p}$ for all p are simultaneously transmitted, the baseband transmitted signal can be written as

$$s(k) = \sum_{p=0}^{P-1} s_p(k) = \frac{1}{\sqrt{M}} \sum_{p=0}^{P-1} \sum_{m=0}^{M-1} \bar{d}_{m,p} e^{j2\pi mk/M}. \tag{8}$$

Then, similar to the classical OFDM, CP is inserted and the transmitted signal gets through the multipath channel. After the CP removal and M-point DFT at the receiver, the demodulation is obtained:

$$\tilde{d}_m = \sum_{p=0}^{P-1} H_m \bar{d}_{m,p} + \eta_m. \tag{9}$$

Note that H_m stands for the channel coefficient for the m -th subcarrier and η_m satisfies the Gaussian distribution.

Subsequently, the single-tap equalization is employed, i.e.,

$$\hat{d}_m = \frac{\tilde{d}_m}{H_m} = \sum_{p=0}^{P-1} \bar{d}_{m,p} + \frac{\eta_m}{H_m}. \tag{10}$$

Based on (5), it is realized that $d_{r,p} = d_{nR+r,p}$ for $n = 0, 1, \cdots, P-1$. Accordingly, the transmitted symbol $d_{r,p}$ can be recovered as

$$\phi_{r,p} = \sum_{n=0}^{P-1} \hat{d}_{nR+r} e^{j2\pi np/P} = \sum_{n=0}^{P-1} \sum_{p_0=0}^{P-1} \bar{d}_{nR+r,p_0} e^{j2\pi np/P} + \sum_{k=0}^{P-1} \frac{\eta_{nR+r} e^{j2\pi np/P}}{H_{nR+r}}. \tag{11}$$

Following (6), equation (11) is rewritten as

$$\phi_{r,p} = \sum_{n=0}^{P-1} \sum_{p_0=0}^{P-1} d_{nR+r,p_0} e^{j2\pi np_0/P} e^{j2\pi np/P} + \xi_{r,p}, \tag{12}$$

where $\xi_{r,p} = \sum_{n=0}^{P-1} \eta_{nR+r} e^{j2\pi np/P} / H_{nR+r}$.

Due to the orthogonality of phase sequences, the following equation holds:

$$\sum_{n=0}^{P-1} e^{j2\pi np/P} e^{j2\pi np_0/P} = \begin{cases} P, & p = p_0, \\ 0, & p \neq p_0. \end{cases} \tag{13}$$

Therefore, it is obtained as

$$\phi_{r,p} = \sum_{n=0}^{P-1} \hat{d}_{nR+r} e^{j2\pi np/P} = P d_{r,p} + \xi_{r,p}. \tag{14}$$

Then, the transmitted symbol can be recovered by

$$\hat{d}_{r,p} = \frac{\phi_{r,p}}{P}. \tag{15}$$

As a remark, when the number of branches is the same as the number of the groups, the data rate of the proposed scheme is the same as that of the classical OFDM. When it is smaller, the data rate of the proposed scheme is smaller than that of the classical OFDM. When it is larger, the orthogonality disappears and the interference is caused.

As two special cases, when $P = 1$, the proposed scheme will be equivalent to the conventional OFDM systems, and when $P = M$, the transmitter of the proposed scheme will be equivalent to the single-carrier frequency domain equalization (SC-FDE) [16]. Note that, due to the signal superposition, the original OFDM signal suffers a large PAPR value, while the SC-FDE signal exhibits a very small PAPR due to the absence of the signal superposition.

4. PAPR Analysis

In this section, we give the theoretical analysis on the PAPR performance. According to (8), the transmitted signal is given as

$$s(k) = \frac{1}{\sqrt{M}} \sum_{p=0}^{P-1} \sum_{m=0}^{M-1} \bar{d}_{m,p} e^{j2\pi mk/M}. \tag{16}$$

Compared with (1), the signal superposition of (16) comes from not only the subcarriers m but also the branches p.

By substituting (6) into (16), the following is obtained:

$$s(k) = \frac{1}{\sqrt{M}} \sum_{p=0}^{P-1} \sum_{r=0}^{R-1} \sum_{\alpha=0}^{P-1} d_{\alpha R+r,p} e^{j2\pi\alpha p/P} e^{j2\pi(\alpha R+r)k/M}. \quad (17)$$

Due to the fact that $d_{\alpha R+r,p} = d_{r,p}$ as equation (5), (17) is rewritten as

$$\begin{aligned} s(k) &= \frac{1}{\sqrt{M}} \sum_{p=0}^{P-1} \sum_{r=0}^{R-1} \sum_{\alpha=0}^{P-1} d_{r,p} e^{j2\pi\alpha p/P} e^{j2\pi(\alpha R+r)k/M} \\ &= \frac{1}{\sqrt{M}} \sum_{p=0}^{P-1} \sum_{r=0}^{R-1} \sum_{\alpha=0}^{P-1} d_{r,p} e^{j2\pi rk/PR} e^{j2\pi\alpha p/P} e^{j2\pi\alpha k/P}. \end{aligned} \quad (18)$$

For the time index k in (18), it is rewritten as

$$k = \beta P + l, \quad (19)$$

where $l = 0, 1, \cdots, R-1$ and $\beta = 0, 1, \cdots, P-1$. Then, (18) is rewritten as

$$\begin{aligned} s(\beta P + l) &= \frac{1}{\sqrt{M}} \sum_{p=0}^{P-1} \sum_{r=0}^{R-1} \sum_{\alpha=0}^{P-1} d_{r,p} e^{j2\pi r(\beta P+l)/PR} \times e^{j2\pi\alpha p/P} e^{j2\pi\alpha(\beta P+l)/P} \\ &= \frac{1}{\sqrt{M}} \sum_{p=0}^{P-1} \sum_{r=0}^{R-1} \sum_{\alpha=0}^{P-1} d_{r,p} e^{j2\pi r(\beta P+l)/PR} \times e^{j2\pi\alpha p/P} e^{j2\pi\alpha l/P} \\ &= \frac{1}{\sqrt{M}} \sum_{p=0}^{P-1} \sum_{r=0}^{R-1} d_{r,p} e^{j2\pi r(\beta P+l)/PR} \times \sum_{\alpha=0}^{P-1} e^{j2\pi\alpha p/P} e^{j2\pi\alpha l/P}. \end{aligned} \quad (20)$$

According to (13), the following equation holds:

$$\sum_{\alpha=0}^{P-1} e^{j2\pi\alpha p/P} e^{j2\pi\alpha l/P} = \begin{cases} P, & p = l, \\ 0, & p \neq l. \end{cases} \quad (21)$$

Then, (20) can be rewritten as

$$s(\beta P + l) = \frac{P}{\sqrt{M}} \sum_{r=0}^{R-1} d_{r,l} e^{j2\pi r(\beta P+l)/PR}. \quad (22)$$

From (22), it is realized that the signal $s(\beta P + l)$ for a certain l is determined only by $d_{m,l}$. In other words, the signals of $d_{m,l}$ and $d_{m,p}$ are nonoverlapping in the time domain for $p \neq l$. For example, the transmitted signals of $d_{m,0}$ are $s(\beta P)$ with $\beta = 0, 1, \cdots, P-1$, while the transmitted signals of $d_{m,1}$ are $s(\beta P + 1)$ with $\beta = 0, 1, \cdots, P-1$. Furthermore, the amplitude of $s(\beta P + l)$ can be obtained as

$$\begin{aligned} |s(\beta P + l)| &= \frac{P}{\sqrt{M}} \left| \sum_{r=0}^{R-1} d_{r,l} e^{j2\pi r(\beta P+l)/PR} \right| \\ &= \frac{P}{\sqrt{M}} \left| \sum_{r=0}^{R-1} d_{r,l} e^{j2\pi rl/PR} e^{j2\pi r\beta/R} \right|. \end{aligned} \quad (23)$$

Defining $\tilde{d}_{r,l} = d_{r,l} e^{j2\pi rl/PR}$, (23) is rewritten as

$$|s(\beta P + l)| = \frac{P}{\sqrt{M}} \left| \sum_{r=0}^{R-1} \tilde{d}_{r,l} e^{j2\pi r\beta/R} \right|. \quad (24)$$

It is clear that the transmitted signal by the proposed scheme is equivalent to the superposition of $R subcarriers, i.e., R-point IDFT. Hence, for an OFDM system with M subcarriers, its PAPR is reduced significantly by the proposed scheme, and specifically, it is equivalent to PAPR of the OFDM system with $R = M/P$ subcarriers.

As a remark, SI is not required in the proposed scheme since the phase sequences are fixed for both the transmitter and receiver, which is different from the conventional SLM method in OFDM systems. In addition, for the conventional SLM method, the optimal phase sequence is chosen by calculating and comparing multiple PAPR values, resulting in the high complexity. However, compared with the classical OFDM, the increase of complexity is mainly from the linear multiplication with phase sequences in the proposed scheme, as equation (6) at the transmitter and equation (12) at the receiver. For both equations (6) and (12), the number of complex-valued multiplications is M. Therefore, the total increased complexity is $2M$ considering both the transmitter and receiver. Note that, for the IDFT operation that can be implemented by IFFT at the transmitter, the complexity is $M \log M$. Compared to the IDFT operation, the increased complexity is acceptable in the proposed scheme due to the reason $M \ll M \log M$.

5. Simulation Results

In this section, simulations are carried out to evaluate the proposed scheme for 5G-IoT, in terms of CCDF and BER. In simulations, the following parameters in 5G NR numerology are employed: subcarrier spacing of 15 kHz, symbol duration of 66.7 μs, CP length of 5.2 μs, and symbol number per time slot of 14. To verify no intersymbol interference in the proposed scheme, no power amplifier is used in the simulations of BER. The detailed parameters of multipath channels are as follows:

(i) Number of paths: 3

(ii) Delay profile (μs): 0, 4, and 10

(iii) Power profile (dB): 0, -5, and -10

Figure 2 depicts BER of the proposed scheme under the additive white Gaussian noise (AWGN) channel and the multi-path channel, respectively. For the proposed scheme, the parameters R and M are set to 16 and 64. The simulation results demonstrate that there is no BER loss with our scheme, which means that the proposed methodology can overcome the multipath fading effectively without the intersymbol interference. It is noted that the existing clipping method suffers obvious BER loss under both the AWGN and multipath channels, which is due to the signal distortion caused by clipping.

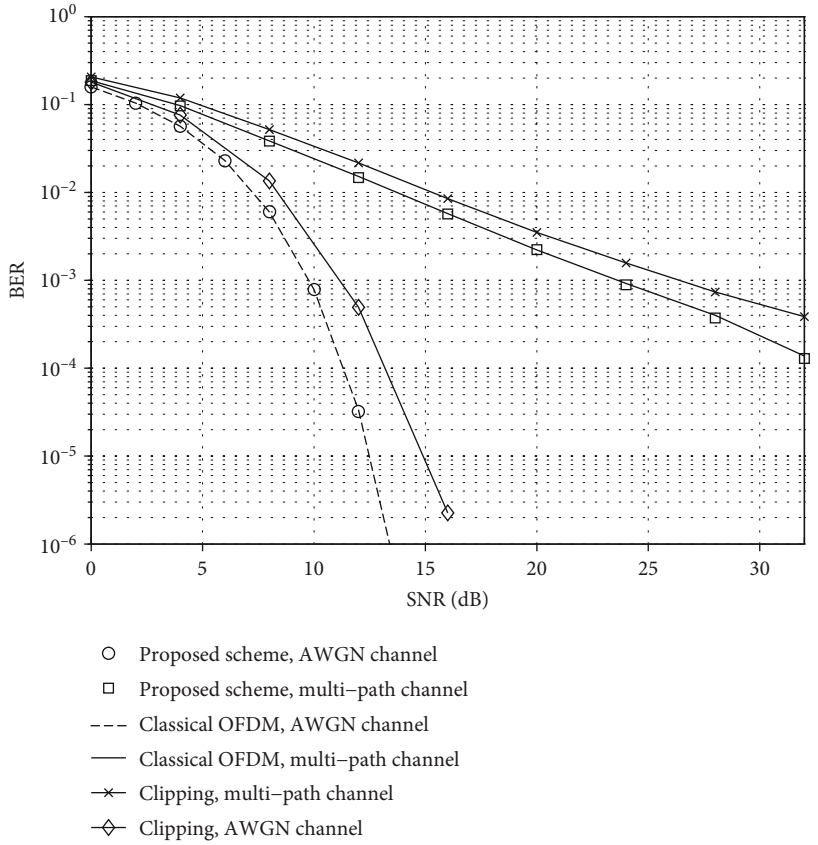

Figure 2: BER of the proposed scheme in OFDM systems for 5G-IoT, $M = 64$, and $R = 16$.

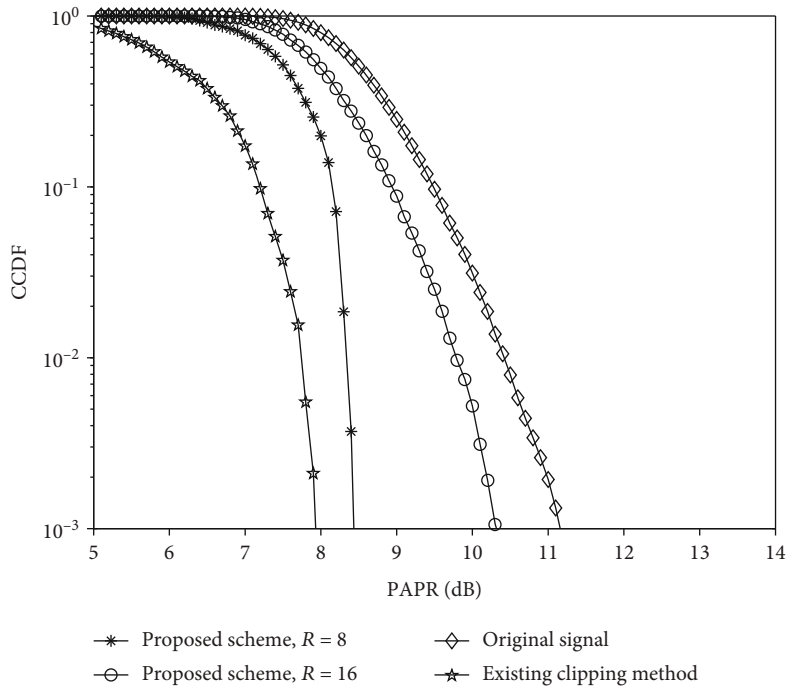

Figure 3: CCDF of the proposed scheme with 4QAM and $M = 64$.

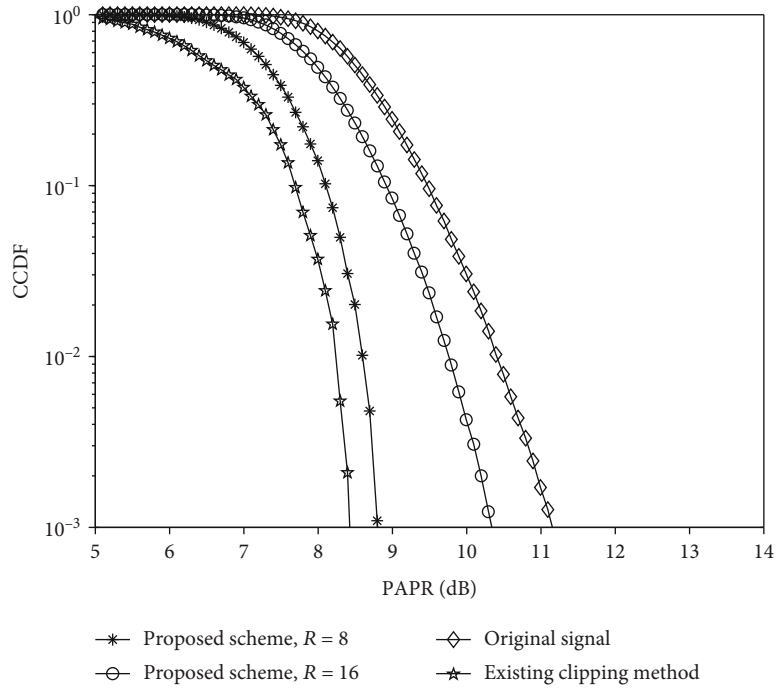

Figure 4: CCDF of the proposed scheme with 16QAM and $M = 64$.

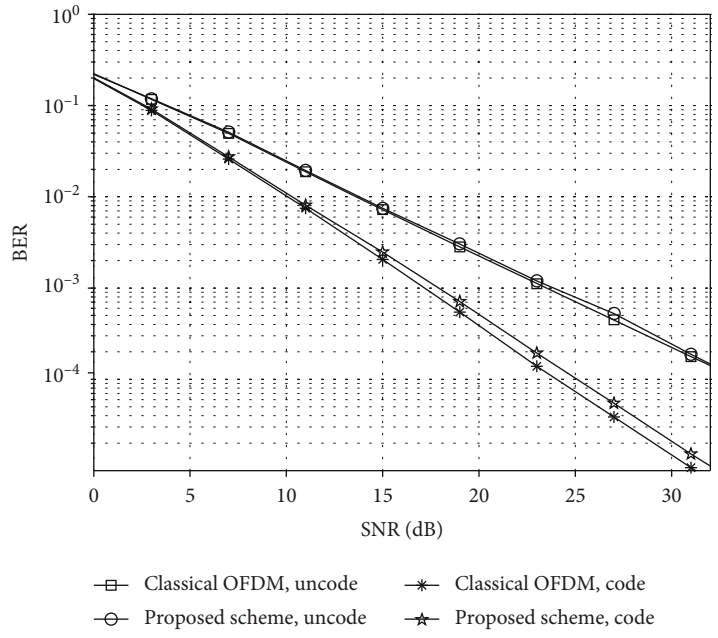

Figure 5: BER of the proposed schemes with channel codes; code rate = 0.5.

As depicted in Figures 3 and 4, the CCDFs of the proposed scheme with 4-QAM (quadrature amplitude modulation) and 16-QAM are, respectively, given under the condition $M = 64$. For comparison, we also give the CCDFs of the existing clipping method, in which no SI is required. Compared with the original signal of the OFDM system, the proposed scheme achieves lower PAPR. Specifically, the proposed scheme with $R = 16$ has about 1 dB gain at CCDF = 10^{-3}, and the proposed scheme with $R = 8$ has about 2.5 dB gain at CCDF = 10^{-3} compared with the original signal. The results are in accordance with the PAPR analysis in Section 4; i.e., the transmitted signal by the proposed scheme is equivalent to the superposition of R subcarriers, i.e., R-point IDFT. Due to the reduction of the IDFT size, PAPR of the OFDM system with M subcarriers can be reduced significantly in the proposed scheme. In addition, it can be observed from Figures 3 and 4 that the existing

clipping method achieves better PAPR performance than the proposed scheme. However, it is noteworthy that, due the signal distortion, the existing clipping method suffers obvious BER loss.

To evaluate the ability of exploiting frequency diversity, Figure 5 shows the BER comparison of uncoded and coded schemes. For comparison, the BER performances of the original OFDM are also given. In simulations, the convolution code with a code rate 0.5 is adopted. From the simulation results, compared with the uncoded scheme, an obvious gain can be achieved in the coded scheme. Therefore, the proposed scheme can also exploit frequency diversity effectively. In addition, it is observed that the coded scheme suffers a bit of BER loss at high SNR compared with the original OFDM. The reason may be that the proposed scheme tends to become a single-carrier modulation as R decreases.

6. Conclusion

In this paper, a novel modulation technique was proposed for 5G-IoT systems by employing the concept of symbol repetition in the frequency domain. It was demonstrated that the proposed scheme significantly reduced the peak power of the transmitted OFDM signal without the signal distortion and SI. Furthermore, it was noted that the number of transmitted symbols could be maintained despite of the design of symbol repetition in the proposed scheme. Numerical simulations have shown the effectiveness of the proposed method.

Data Availability

The data used to support the findings of this study are available from the corresponding author upon request.

Conflicts of Interest

The authors declare that there are no conflicts of interest regarding the publication of this paper.

Authors' Contributions

Junchao Sun and Buyu Chen contributed equally to this work.

Acknowledgments

This work was financially supported in part by the National Science Foundation of China with Grant number 62001333.

References

[1] H. Zhang, N. Liu, X. Chu, K. Long, A. Aghvami, and V. Leung, "Network slicing based 5G and future mobile networks: mobility, resource management, and challenges," *IEEE Communications Magazine*, vol. 55, no. 8, pp. 138–145, 2017.

[2] D. Kong, X.-G. Xia, P. Liu, and Q. Zhu, "MMSE channel estimation for two-port demodulation reference signals in new radio," *SCIENCE CHINA Information Sciences*, vol. 64, pp. 169303:1–169303:2, 2021.

[3] D. Kong, Y. Xu, G. Song, J. Li, and T. Jiang, "A CP reduction scheme based on symbol repetition for narrow-band IoT systems," *IEEE Internet of Things Journal*, vol. 8, no. 16, pp. 12880–12891, 2021.

[4] J.-Y. Woo, H. S. Joo, K.-H. Kim, J.-S. No, and D.-J. Shin, "PAPR analysis of class-III SLM scheme based on variance of correlation of alternative OFDM signal sequences," *IEEE Communications Letters*, vol. 19, no. 6, pp. 989–992, 2015.

[5] L. Yang, R. S. Chen, Y. M. Siu, and K. K. Soo, "PAPR reduction of an OFDM signal by use of PTS with low computational complexity," *IEEE Transactions on Broadcasting*, vol. 52, no. 1, pp. 83–86, 2006.

[6] X. Li and L. J. Cimini, "Effects of clipping and filtering on the performance of OFDM," *IEEE Communications Letters*, vol. 2, no. 5, pp. 131–133, 1998.

[7] L. Wang and C. Tellambura, "Analysis of clipping noise and tone-reservation algorithms for peak reduction in OFDM systems," *IEEE Transactions on Vehicular Technology*, vol. 57, no. 3, pp. 1675–1694, 2008.

[8] W. Hu, W. Huang, Y. Ciou, and C. Li, "Reduction of PAPR without side information for SFBC MIMO-OFDM systems," *IEEE Transactions on Broadcasting*, vol. 65, no. 2, pp. 316–325, 2019.

[9] S.-C. Lim, N. Kim, and H. Park, "Polar coding-based selective mapping for PAPR reduction without redundant information transmission," *IEEE Communications Letters*, vol. 24, no. 8, pp. 1621–1625, 2020.

[10] T. Arbi, Z. Ye, and B. Geller, "Low-complexity blind PAPR reduction for OFDM systems with rotated constellations," *IEEE Transactions on Broadcasting*, vol. 67, no. 2, pp. 491–499, 2021.

[11] S. Gopi and S. Kalyani, "An optimized SLM for PAPR reduction in non-coherent OFDM-IM," *IEEE Wireless Communications Letters*, vol. 9, no. 7, pp. 1–971, 2020.

[12] H. Wang, P. Xiao, and X. Li, "Channel parameter estimation of mmwave MIMO system in urban traffic scene: a training channel-based method," *IEEE Transactions on Intelligent Transportation Systems*, pp. 1–9, 2022.

[13] H. Wang, L. Xu, Z. Yan, and T. A. Gulliver, "Low-complexity MIMO-FBMC sparse channel parameter estimation for industrial big data communications," *IEEE Transactions on Industrial Informatics*, vol. 17, no. 5, pp. 3422–3430, 2020.

[14] D. Kong, X. Zheng, Y. Zhang, and T. Jiang, "Frame repetition: a solution to imaginary interference cancellation in FBMC/OQAM systems," *IEEE Transactions on Signal Processing*, vol. 68, pp. 1259–1273, 2020.

[15] D. Kong, D. Qu, and T. Jiang, "Time domain channel estimation for OQAM-OFDM systems: algorithms and performance bounds," *IEEE Transactions on Signal Processing*, vol. 62, no. 2, pp. 322–330, 2014.

[16] X. Cheng, Y. Yang, and S. Q. Li, "Joint compensation of transmitter and receiver I/Q imbalances for SC-FDE systems," *IEEE Transactions on Vehicular Technology*, vol. 69, no. 8, pp. 8483–8498, 2020.